PHYSICAL REVIEW B VOLUME 53, NUMBER 21 1 JUNE 1996-I

Ferroelastic phase transitions in the $K_3Na(SeO_4)_2$ glaserit-type crystal

J. Díaz-Hernández, J. L. Mañes, M. J. Tello, and A. López-Echarri
Departamento de Física de la Materia Condensada, Facultad de Ciencias, Universidad del Pais Vasco, Euskal Herriko Unibersitatea, Apartado 644 Bilbao, 48080, Spain

T. Breczewski and I. Ruiz-Larrea
Departamento de Física Aplicada II, Facultad de Ciencias, Universidad del Pais Vasco, Euskal Herriko Unibersitatea, Apartado 644 Bilbao, 48080, Spain

(Received 31 October 1995)

Successive structural phase transitions in $K_3Na(SeO_4)_2$ at $T_c \approx 329$ K and $T_0 \approx 346$ K were studied by adiabatic calorimetry, thermal expansion, linear birefringence, differential scanning calorimetry, and optical observations of domains. The experimental results in this paper together with x-ray and elastic measurements in the literature are interpreted by means of a theoretical model based on the Landau phenomenological approach. This model gives a $P\bar{3}m1 \xrightarrow{346\ \mathrm{K}} B2/m \xrightarrow{329\ \mathrm{K}} C2/c$ phase transition sequence with second (346 K) and first (329 K) character, respectively. Because of histeresis effects, the intermediate phase tends to appear as a mixture of both monoclinic phases. [S0163-1829(96)01118-6]

I. INTRODUCTION

Among the compounds with an $A_3C(BX_4)_2$ general formula, where A, C=Li, Na, K, Rb, and Cs and BX_4 tetrahedra=SO_4, SeO_4, and CrO_4, the $K_3Na(BO_4)_2$ subfamily (KNB for short), the members of which show the glaserit structure $(3m)$, remains a subject of traditional investigation for ferroelastic phase transitions.[1–6] Two members of this subfamily with B=Cr (KNCr) and Se (KNSe) show some common features: (1) A hexagonal $6/mmm$ structure at high temperature; (2) the presence of ferroelasticity, but the absence of other types of properties related to structural change such as piezoelectricity, ferroelectricity, or piroelectricity; (3) order-disorder structural phase transition sequences which seem to be a consequence of the spatial ordering of the tetrahedra in the crystal lattice. This sequence for KNCr compounds is ($6/mmm \rightarrow$unknown$\rightarrow 3m \rightarrow 2/m$), but it was pointed out that KNSe probably has a different phase transition sequence.[1,4]

X-ray studies show that KNSe presents a glaserit $(\bar{3}m)$ structure above 346 K.[3] However, when the temperature is lowered, different phase transition sequences were suggested, depending on which experimental technique was used. High-resolution Brillouin spectroscopy[1] suggests a phase transition at 346 K involving an unknown Q mode followed by a $3m \rightarrow 2/m$ phase transition at 329 K. Macroscopic measurements (thermal, elastic, and dielectric) as well as optical observations of domain structures[4] suggest two improper structural phase transitions at 346 and 329 K. This last temperature has been adopted conventionally, since its actual value is somewhat uncertain due to histeresis effects. In this case the point-group sequence proposed was $3m \rightarrow 3m \rightarrow 2/m$. Based on recent x-ray results, the space-group sequence $P3m1 \rightarrow P3c1 \rightarrow (P2_1/a,\ P2/a,\ \text{or}\ C2/c)$ was proposed in the same paper.[4]

An analysis of the theoretical and experimental results in Refs. 1 and 4 shows that the phase transition sequences of KNSe are far from being well understood. A phenomenological approach using an effective free energy which involves a coupling term between the $3m \rightarrow 2/m$ order parameter and an additional $3m \rightarrow 3m$ mode Q was carried out in Ref. 1. In this approach the order parameter Q was introduced without any symmetry arguments. As we shall see later, additional x-ray measurements as well as new experimental results seem to be in disagreement with this phenomenological approach.

The purpose of this paper is to give an insight into the experimental and theoretical description of the phase transition sequences in this interesting glaserit type of crystal. Various experimental techniques such as adiabatic calorimetry, birefringence, thermal expansion, and optical observations of domains in the temperature range from 290 to 380 K have been used. Experimental techniques are described in Sec. II, whereas the experimental results are examined in Sec. III. A theoretical analysis is carried out in Sec. IV, where a model based on the Landau phenomenological approach which explains the ferroelastic phase transition sequence in this crystal is presented.

II. EXPERIMENTAL DETAILS

Single crystals of $K_3Na(SeO_4)_2$ were grown from a saturated, aqueous, stoichiometric solution by the steady-state method[7] at 305 K. Chemically pure K_2SeO_4 and Na_2SeO_4 stock reagents were used for synthesis. The synthesis product was purified by recrystallization using distilled water. The obtained crystals of size $1.0 \times 1.0 \times 1.0\ \mathrm{cm}^3$ were colorless, transparent, and of good optical quality. Their chemical composition was confirmed by atomic spectroscopy. Samples of three different orientations were prepared from untwinned parts of the crystal in order to study the physical properties. The heat capacity measurements were made with an adiabatic calorimeter previously described.[8] The calibration of the experimental system gives a C_p accuracy better than 0.1% throughout the whole measured temperature range

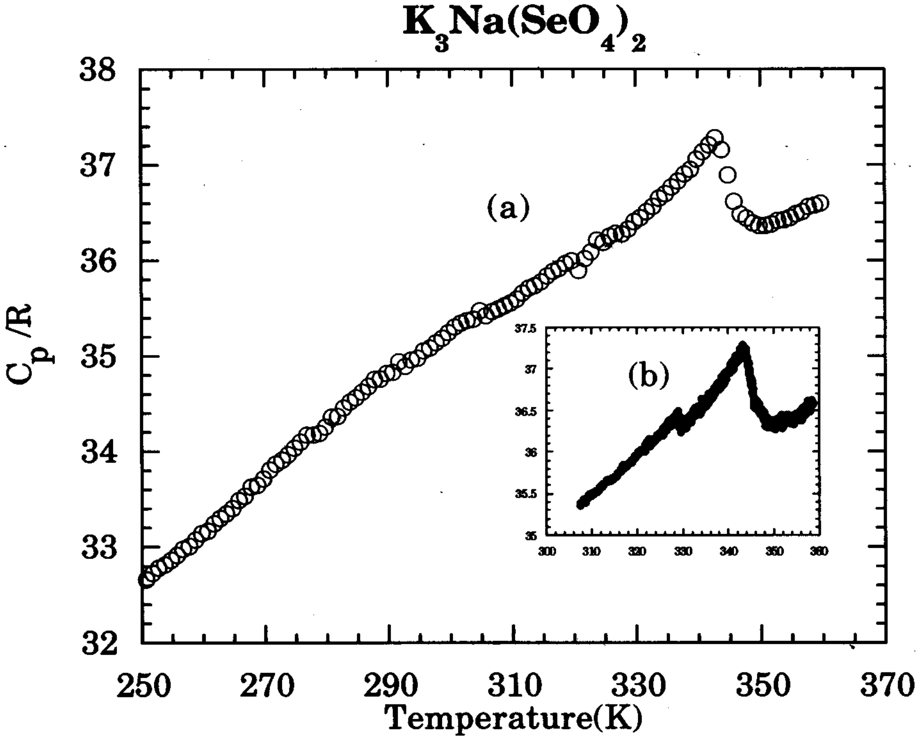

FIG. 1. Experimental specific heat of $K_3Na(SeO_4)_2$ obtained by means of the discontinuous pulse technique. The heating rate was 6 K/h; the inset shows the superposition of two measurements obtained by continuous heating method (thermogram) with heating rates of 2 and 2.5 K/h. Two specific heat anomalies were observed at 329 and 346 K.

(20–360 K), and the temperature control is better than 1 mK. 94.2364 g of the powder sample of KNSe were used to fill the calorimeter vessel. Low-pressure (10 mm Hg at room temperature) helium gas was added in the sample vessel as a heat interchange, which provides short equilibrium times after each heating period. Two measuring methods were used: the discontinuous heating procedure (pulse) and the thermogram technique. Birefringence measurements were made using two experimental techniques: an authomatic Senarmont method, which allows a direct recording of the optical path against temperature, and the classical compensator method using a polarizing microscope with a cooling setup. The same microscope was used for the measurement of the optical axis and angle (E or V) for the optical observation of ferroelastic domains. Thermal expansion was measured using a standard dilatometer in the conditions of dynamic temperature changes. Cooling and heating measurements were carried out with rates of 1 and 2 °C/min along the three main crystallographic axes.

III. EXPERIMENTAL RESULTS

Figure 1 shows the specific heat curve (a) in the 250–365 K temperature interval. The experimental points were obtained by the discontinuous heating method. A clear specific heat anomaly can be observed at 346 K which is similar to those depicted in Ref. 4. On the other hand, we have noticed small anomalies in the equilibrium times around 329 K. These anomalies appear at the same temperature in the specific heat curve. In order to define more accurately the shape of the specific heat curve and analyze the anomalous thermal relaxation times interval, three independent thermograms were made between 310 and 360 K. The results in Fig. 1 [curve (b)] show a new specific heat anomaly at 329 K. This anomaly is in agreement with those detected by direct observations of domain structures and softening of some elastic moduli in Refs. 1 and 4. The values of the thermodynamic functions for these phase transitions were determined with the help of an approximate specific heat base line by extrapolation of the low-temperature specific heat curve. This approximation was necessary because we have not sufficient spectroscopic information at this moment. Using numerical integration we obtained the following values for the phase transition thermodynamic functions: [$\Delta H/(RK)=0.586$ and $\Delta S/R=0.0019$] for the first phase transition and [$\Delta H/(RK)=17.63$ and $\Delta S/R=0.05$] for the phase transition at 346 K (see Table I).

Figure 2 shows the optical path measurements along the [0,0,1] direction in the temperature range 300–353 K. The experimental values show that the birefringence goes to zero above the phase transition at 346 K. The continuous change in the optical path curve together with the absence of thermal hysteresis confirms the second-order character for this phase transition in agreement with the specific heat curves in Fig. 1. This result is in disagreement with a previous theoretical model[1] which considered a $\bar{3}m \rightarrow 3m$ phase transition at this temperature. A small anomaly at 329 K is in agreement with those showed in the specific heat curves (Fig. 1) at the same temperature. Both results confirm, in agreement with other experimental results,[1,4] the existence of the new phase transition at 329 K. However, in this case, both distorted phases

TABLE I. Temperature, enthalpy, and entropy associated with the two phase transitions in $K_3Na(SeO_4)_2$.

Temperature (K)	$\Delta H/(RK)$	$\Delta S/R$
$T_1=346$	17.63	0.05
$T_2=329$	0.586	0.0019
Total sequence	18.22	0.052

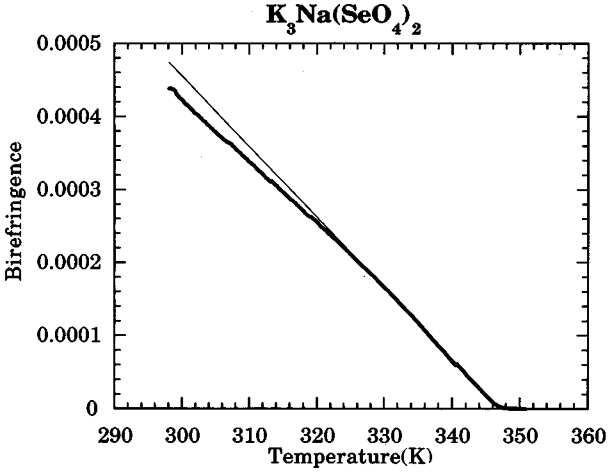

FIG. 2. Temperature dependence of the birefringence (Δn) of $K_3Na(SeO_4)_2$ measured along the c axis.

show birefringence, which is in disagreement with the previously proposed $3m \rightarrow 3m \rightarrow 2/m$ sequence.[1] These optical results are confirmed in Fig. 3, where we show the optical angle $[V(T)]$.[9] $V(T)$ is a function of the temperature dependence of the birefringence and the thermal expansion. Therefore, in the framework of the Landau theory for ferroelastic crystals, $V(T)$ is given by a complicated, but continuous function of the order parameter. In this way the curve in Fig. 3 shows a second-order phase transition at 346 K from a nonbirefringent to a birefringent phase.

In order to clarify the intermediate structure between the high-temperature hexagonal structure and the monoclinic $(2/m)$ phase, both confirmed with previous x-ray measurements, we have carried out a careful domain observation. Ferroelastic domains structure and conoscopic figures for the crystal plates oriented in the [001] direction were made in the temperature range from 290 up to 370 K. The ferroelastic domain walls observed in the temperature range from room temperature up to 329 K have orientations characteristic for the crystal with the $3mF2/m$ ferroelastic phase transition.[10] The domain wall orientation may be described as $Y=0$ and $Y=\pm\sqrt{3}X$.[7] The application of a small shear stress causes the domain walls to move.

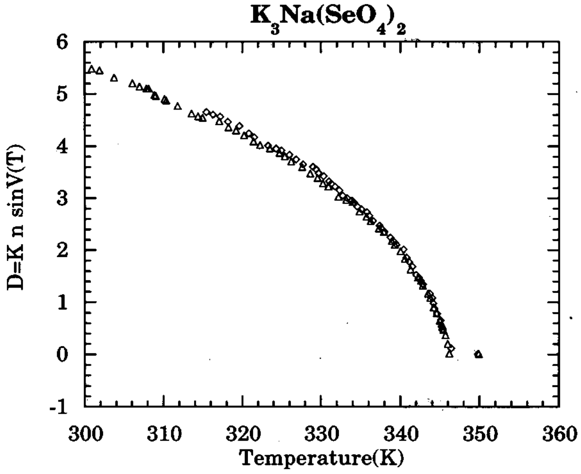

FIG. 3. Temperature dependence of the optic angle of $K_3Na(SeO_4)_2$. The optical angle $V(T)$ is given by $D=Kn\sin V(T)$, where D is half the scalar distance between the optic axes, n is the index of refraction, and K is Mallard's constant (see Ref. 9). These measurements confirm the second-order character for the phase transition at 346 K.

In the temperature region 329–348 K the image of the domain structure becomes blurred, confused, and highly dependent on the thermal history of the sample. The coexistence of the extinction zones at 90° (Ref. 7) with the domain structure present up to 329 K has also been observed. Above $T=346$ K the domain structure pattern observed for this crystalographic direction of crystal samples has disappeared.

In agreement with the birefringence measurements, images typical for a biaxial crystal were observed in the whole temperature range from room temperature up to 348 K using the conoscopic method in a monodomain zone of the sample.

The thermal expansion measurements were carried out on a crystal oriented along the three main crystallographic directions. The experimental results together with the thermal expansion coefficients are given in Fig. 4. The results are in agreement with those in Ref. 4 for α_3 and show some discrepancies for α_1 and α_2. The experimental results in Fig. 4 show a clear phase transition in the α_3 curve, but no anomalies are present at 329 K. This fact is in complete agreement with the theoretical model in the next section, where we obtain that for some crystallographic directions the thermal expansion effects tend to cancel out. This result is also in agreement with the domain observations.

IV. PHENOMENOLOGICAL THEORY

Previous phenomenological models for the trigonal →monoclinic ferroelastic phase transitions in $K_3Na(SeO_4)_2$ (Ref. 1) and $K_3Na(CrO_4)_2$ (Ref. 2) were based solely on the knowledge of the point-group symmetries. In both cases the change is $3m \rightarrow 2/m$, which was attributed to the Γ point ($\mathbf{K}=0$) two-dimensional representation E_g. An additional order parameter of unspecified symmetry was added to the model in an attempt to explain the two successive phase transitions observed in $K_3Na(SeO_4)_2$.

More recently, the structure of $K_3Na(SeO_4)_2$ has been obtained at $T=390$ and 291 K. According to Ref. 3, the high- and low-temperature space groups are given by $P3m1$ and $C2/c$, respectively, with the OZ axis doubling its length in the monoclinic phase. This reduction in the translational symmetry requires a representation with $\mathbf{K}\neq 0$. Standard group theoretical considerations show that there are only two possibilities. We can have a combination $E_g(q_1,0)+A_2^+(Q)$, where A_2^+ is an irreducible representation (IR) at the A point ($\mathbf{K}=\frac{1}{2}\mathbf{g}_1$; see Ref. 11 for notation) of the first Brillouin zone and E_g is the Γ-point two-dimensional IR mentioned above. The order parameter components which are nonzero in the low-symmetry phase are indicated between brackets:

$$P\overline{3}m1 \xrightarrow{E_g(q_1,0)+A_2^+(Q)} C2/c. \qquad (1)$$

Alternatively, the transition can be explained by a single two-dimensional IR $A_3^+(0,q_2)$ at the A point:

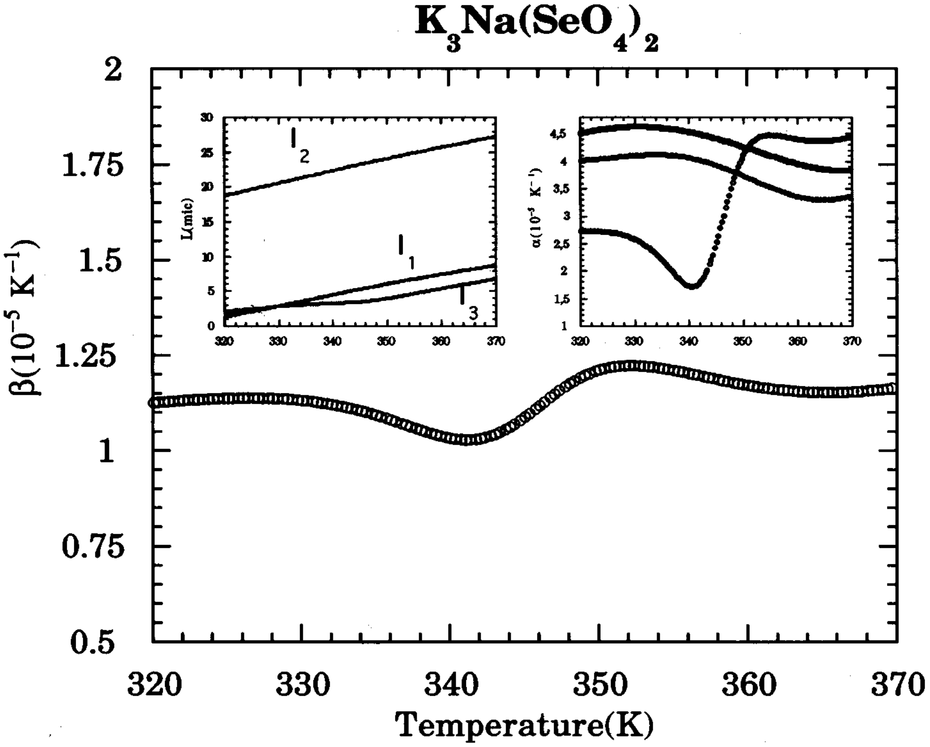

FIG. 4. Volume expansion coefficient β as a function of temperature. The inset shows the thermal elongation and expansion α_i $(i=1,2,3)$ along the three main crystallographic axes, obtained by the standard push-rod dilatometric method. Measurements were carried out with cooling and heating rates of 1 and 2 °C/min.

$$P\bar{3}m1 \xrightarrow{A_3^+(0,q_2)} C2/c. \tag{2}$$

Depending on which of the order parameters is activated first, there are two possible sequences associated with (1):

$$P\bar{3}m1 \underset{\text{second order}}{\xrightarrow{A_2^+(Q)}} P\bar{3}c1 \underset{\text{first order}}{\xrightarrow{E_g(q_1,0)}} C2/c, \tag{3a}$$

$$P\bar{3}m1 \underset{\text{first order}}{\xrightarrow{E_g(q_1,0)}} B2/m \underset{\text{second order}}{\xrightarrow{A_2^+(Q)}} C2/c. \tag{3b}$$

The A_2^+-phase transition may be continuous, whereas the one corresponding to E_g must necessarily be of first order. Since the intermediate phase is observed to be monoclinic, the sequence in (3b) seems to be selected. However, the trigonal→monoclinic transition shows a very marked second-order character, which is incompatible with the existence of a cubic invariant for E_g.[12]

This difficulty disappears if one considers instead the representation A_3^+ in (2). Since $\mathbf{K}\neq\mathbf{0}$, but $2\mathbf{K}\equiv\mathbf{0}$, only even-degree invariants are allowed, and the transition can be continuous. (One can easily check that Lifshitz's condition for the existence of a second-order phase transitions[12] is also fulfilled.) This solves the problem of explaining the second-order trigonal→monoclinic phase transition at $T_0\approx 346$ K. However, we still have to account for the very weak monoclinic→monoclinic phase transition observed at $T_c\approx 329$ K. This can be done very naturally by noting that $A_3^+(q_1,0)$ takes us from $P\bar{3}m1$ to $B2/m$:

$$P\bar{3}m1 \underset{\text{second order}}{\xrightarrow{A_3^+(q_1,0)}} B2/m \underset{\text{first order}}{\xrightarrow{A_3^+(0,q_2)}} C2/c. \tag{4}$$

Since the order parameter ''jumps'' from $(q_1,0)$ to $(0,q_2)$ at $T=329$ K, this phase transition is necessarily first order. Also note that unlike in (3b) the doubling along the OZ axis takes place during the trigonal→monoclinic phase transition at 346 K.

In order to construct the free energy corresponding to (4), it is convenient to use polar coordinates $(q_1,q_2)\equiv q(\cos\theta,\sin\theta)$. The only quartic invariant (q^4) is isotropic, and we have to include higher-order terms. These are two sixth-order invariants q^6 and $q^6\cos 6\theta$. If the coefficient of $q^6\cos 6\theta$ is negative, $(q_1,0)$ will be a minimum and $(0,q_2)$ a maximum. At $T_c\approx 329$ K the situation must be reversed. This will happen if the coefficient of the eighth-order invariant $q^8\cos 6\theta$ is positive, since this term will eventually dominate as q^2 increases. We thus consider the free energy

$$\Phi_q=\tfrac{1}{2}\alpha q^2+\tfrac{1}{4}q^4+\tfrac{1}{6}\gamma(\theta)q^6+\tfrac{1}{8}\rho(\theta)q^8, \tag{5}$$

where $\alpha=a(T-T_0)$ with $a>0$, and

$$\gamma(\theta)=\gamma_0-\gamma_1\cos 6\theta, \quad \rho(\theta)=\rho_0+\rho_1\cos 6\theta,$$

with γ_0, ρ_1, ρ_0, and ρ_1 positive and $\rho_0>\rho_1$. The quartic term coefficient has been normalized by a rescaling of the order parameter. Note that, as usual in Landau's phenomenological description of structural phase transitions, only the temperature dependence of the second-degree term $\alpha(T)$ has been taken into account. Rather than by an explicit change of sign for the anisotropic sixth-degree term, the sequence of transitions is caused by the fact that the coefficient of sixth- and eighth-degree anisotropic terms have *constant but opposite* signs.

The monoclinic→monoclinic transition temperature T_c can be found by imposing $\Phi_q(\theta=0)=\Phi_q(\theta=\pi/2)$. This cannot be solved explicitly due to the presence of sixth- and eighth-order terms in (5). However, we can give an approximate expression for T_c if we assume that $q^2(T_c)\equiv q_c^2$ is "small," in the sense that higher-order terms are relatively unimportant, i.e., if $|\gamma(\theta)q_c^2|\ll 1$ and $|\rho(\theta)q_c^2|\ll 1$. This is supported by the facts that only 10°–12° separate the two phase transitions and that the very weak specific heat anomaly at $T_c\approx 329$ K "rides" on the anomaly at $T\approx 346$ K. Under these assumptions we find

$$T_c\approx T_0-\frac{4}{3}\frac{\gamma_1^2}{a\rho_1}, \tag{6}$$

which is valid for $\gamma_0\gamma_1\ll\rho_1$. Similarly, the change in the norm of q^2 at T_c is given by

$$\frac{\delta q^2}{q^2}\equiv\frac{q_2^2-q_1^2}{q_1^2}\approx\frac{8}{9}\frac{\gamma_1^2}{\rho_1^2}\ll 1. \tag{7}$$

Since the entropy is proportional to q^2,

$$S=-\frac{\partial\phi_q}{\partial T}=-\frac{1}{2}aq^2, \tag{8}$$

Eq. (7) implies a very small latent heat for the phase transition at 329 K. This is consistent with calorimetric studies of the material. Note that in this approximation the minima of (5) are given by

$$q^2\approx a(T_0-T),\quad \theta=n\frac{\pi}{3},\quad n=0-5\quad\text{for } T_c<T<T_0, \tag{9a}$$

$$q^2\approx a(T-T_0)+\delta q^2,\quad \theta=\frac{\pi}{2}+n\frac{\pi}{3},$$

$$n=0-5\quad\text{for } T<T_c. \tag{9b}$$

Different values of θ correspond to different domains. In order to describe the effect of the phase transitions on the elastic properties of the crystal, we consider the dependence of the free energy on the strains $\{e_i\}$:

$$\Phi=\Phi_q+\Phi_e+\Phi_{q-e}. \tag{10}$$

Here Φ_q is given by (5) and Φ_e is[13]

$$\begin{aligned}\Phi_e&=\tfrac{1}{4}(C_{11}^0+C_{12}^0)(e_1+e_2)^2+\tfrac{1}{2}C_{33}^0e_3^2+C_{13}^0e_3(e_1+e_2)\\&\quad+\tfrac{1}{4}C_{44}(e_4^2+e_5^2)+\tfrac{1}{4}(C_{11}^0-C_{12}^0)[(e_1-e_2)^2+e_6^2]\\&\quad+C_{14}^0[e_4(e_1-e_2)+e_5e_6].\end{aligned} \tag{11}$$

The behavior of the physical magnitudes is dominated by the lowest-order couplings with the order parameter. These are of the form q^2e:

$$\begin{aligned}\Phi_{q-e}&=\tfrac{1}{2}\mu_1q^2(e_1+e_2)+\tfrac{1}{2}\mu_3q^2e_3\\&\quad+\tfrac{1}{2}\mu_4(e_4\cos2\theta-e_5\sin2\theta)\\&\quad+\tfrac{1}{6}\mu_6[(e_1-e_2)\cos2\theta-e_6\sin2\theta].\end{aligned} \tag{12}$$

There are also 13 coupling terms of the form q^2e^2. Their effect is less important, and they will not be written explicitly. Miniminization of (10) with respect to e_i yields

$$e_i\approx-\tfrac{1}{2}q^2\sum_{j=1}^{6}S_{ij}^0\lambda_j,\quad T<T_0, \tag{13}$$

where $S_{ij}=C_{ij}^{-1}$ and

$$\lambda_1=\mu_1+\mu_6\cos2\theta,\quad \lambda_2=\mu_1-\mu_6\cos2\theta,\quad \lambda_3=\mu_3,$$

$$\lambda_4=\mu_4\cos2\theta,\quad \lambda_5=-\mu_4\sin2\theta,\quad \lambda_6=-\mu_6\sin2\theta. \tag{14}$$

Using (13), (15), and the symmetries of S_{ij}^0, we can give explicit expressions for e_1, e_2, and e_3, which have been studied experimentally:

$$e_1+e_2\approx Aq^2,\quad e_3\approx Bq^2,\quad e_1-e_2\approx Cq^2\cos2\theta, \tag{15}$$

where $A=-(S_{11}^0+S_{12}^0)\mu_1-S_{13}^0\mu_3$, $B=-S_{13}^0\mu_1-\tfrac{1}{2}S_{33}^0\mu_3$, and $C=-(S_{11}^0-S_{12}^0)\mu_6-S_{14}^0\mu_4$. Notice that e_1-e_2 depends on cos 2θ, which reverses its sign at $T_c\approx 334$ K [see Eq. (9)]. As a consequence, the optical indicatrix will turn 90° at that temperature. This will cause the coexistence of extinction zones at 90°. This is in agreement with our optical observations and also explains the image in Fig. 6 of Ref. 7.

Elastic measurements on polydomain samples will tend to average over q. Assuming equal contributions from the three types of ferroelastic domains, we have $\langle\cos 2\theta\rangle=\langle\sin 2\theta\rangle=0$. In particular, the anomaly in e_1-e_2 at T_c will be difficult to detect in elastic expansion measurements. This is consistent with the experimental results. Moreover, since $\delta q^2\ll q^2$, the transition at T_c will have little influence on the expansion coefficients.

The main anomaly in the elastic constants is given by

$$C_{ij}=C_{ij}^0-\tfrac{1}{2}\lambda_i\lambda_j,\quad T<T_0. \tag{16}$$

This implies a discontinuous behavior at T_0, even for a second-order phase transition. Note that for $i=j$ we have a drop in C_{ii}. This is consistent with the measured curves for C_{ii} in Refs. 1 and 4, but not with the temperatures at which the anomalies are supposed to be observed. However, since the results in Refs. 1 and 4 are mutually inconsistent to a great extent, the experimental situation is still unclear in this respect.

Equation (16) gives only the main anomaly in the elastic constant. If one includes the 13 e^2q^2 terms neglected in (12), we find an additional temperature dependence in C_{ij}, proportional to q^2. This dependence is domain independent for the six elastic constants compatible with $3m$, but is a function of θ for the seven remaining constants compatible only with $2/m$. These last will tend to average to zero in polydomain samples, and the anomaly at T_c will show only through the change in q^2, Eq. (7).

The structure of $K_3Na(CrO_4)_2$ at $T=290$ and 230 K has been recently determined.[14] Since the space groups for the trigonal ($T\geq T_c\sim 239$ K) and monoclinic ($T<T_c$) phase are given by $P3m1$ and $C2/c$, respectively, our model can be used for this material as well. If ρ_1 in (5) is negative, only one phase transition will take place.

V. CONCLUSIONS

The following conclusions concerning the structural phase transitions occurring in KNSe can be drawn.

(I) Our experimental results confirm the existence of two structural phase transitions at temperatures 346 and 329 K in KNSe. This last temperature has been adopted conventionally, since its actual value is somewhat uncertain due to histeresis effects.

(II) The intermediate phase is optically biaxial and, due to histeresis effects, tends to appear as a mixture of two monoclinic phases. This explains the coexistence of extinction zones at 90°.

(III) Our theoretical model based on Landau's phenomenological approach predicts a second- (first-) order character for the phase transition at 346 K (329 K) and a monoclinic $B2/m$ symmetry for the intermediate phase. Calorimetric, thermal expansion, optical, and elastic constant measurements are consistent with our phenomenological model.

ACKNOWLEDGMENTS

This work was partially supported by the University of Basque Country Grant Nos. UPV-EHU 063.310-EB119/92 and UPV-EHU 063.310-EB109/92, and by CICYT Grant No. AEN-93-1435. The authors would like to thank Dr. A. Gómez-Cuevas and Dr. E. H. Bocanegra (University of the Basque Country, Spain) for the work carried out using complementary experimental techniques. One of the authors (J.D.-H.) wishes to gratefully acknowledge Universidad Autónoma de Puebla (México) and also CONACYT-México for financial support.

---

[1] B. Mróz, H. Kiefte, M. J. Clouter, and J. A. Tuszynski, Phys. Rev. B **46**, 8717 (1992).

[2] B. Mróz, H. Kiefte, M. J. Clouter, and J. A. Tuszynski, Phys. Rev. B **43**, 641 (1991).

[3] J. Fabry, T. Breczeuski, and V. Petricek, Acta Crystallogr. B **49**, 826 (1993).

[4] T. Krajewski, P. Piskunowicz, and B. Mróz, Phys. Status Solidi A **135**, 557 (1993).

[5] Y. Makita, A. Sawada, and Y. Takagi, J. Phys. Soc. Jpn. **41**, 167 (1976).

[6] B. Mróz, J. A. Tuszynski, H. Kiefte, and M. J. Clouter, J. Phys. Condens. Matter **1**, 5965 (1989).

[7] T. Krajewski, P. Piskunowicz, and B. Mróz, Ferroelectrics **159**, 161 (1994).

[8] J. Zubillaga, A. López-Echarri, and M. J. Tello, Thermochim. Acta **92**, 283 (1985).

[9] Ernest E. Wahlstrom, *Optical Crystallography*, 4th ed. (Wiley, New York, 1969).

[10] J. Sapriel, Phys. Rev. B **12**, 5128 (1975).

[11] C. Bradley and A. P. Cracknell, *The Mathematical Theory of Symmetry in Solids* (London Press, Oxford, 1972).

[12] L. D. Landau and E. M. Lifshitz, *Statistical Physics* (Pergamon, Oxford, 1980).

[13] P. Toledano, M. M. Fejer, and B. A. Auld, Phys. Rev. B **27**, 5717 (1983).

[14] J. Fabry, T. Breczewski, and G. Madariaga, Acta Crystallogr. B **50**, 13 (1994).